International Journal of Advanced Research Trends in Engineering and Technology (IJARTET)
Vol. 1, Issue 3, November 2014

Synchronization of EEG: Bivariate and Multivariate Measures

Sujithra Jenifer.M[1], Antony Gnana Anusiya.S[2], Nancy Lydia.T[3]
Department of Information Technology, Francis Xavier Engineering College, Tirunelveli, India[1]
Department of Information Technology, Francis Xavier Engineering College, Tirunelveli, India[2]
Assistant Professor, Department of Information Technology, Francis Xavier Engineering College, Tirunelveli, India[3]

Abstract: Electroencephalographic (EEG) signals is important for decoding information processing in the human brain, synchronization in pairs of EEG signals to whole brain synchronization maps. Then it can be based on bivariate measures averaging over pair wise values or, alternatively, on multivariate measures, which directly ascribe a single value to the synchronization in a group. In order to compare BM and MM, we applied nine different estimators to simulated multivariate time series with known parameters and to real EEGs. We found widespread correlations between BM and MM, which were almost frequency independent for all the measures except coherence. The analysis of the behavior of synchronization measures in simulated settings with variable coupling strength, connection probability, and parameter mismatch showed that some of them, including S-estimator, S-Renyi, omega, and coherence, are more sensitive to linear interdependences, like mutual information and phase locking value, are more responsive to nonlinear effects. One must consider these properties together with the fact that MM are computationally less expensive and, more efficient for the large scale data sets than BM while choosing a synchronization measure for EEG analysis.

Keywords: Bivariate Measures (BM), Coupled Oscillators, ElectroEncephaloGram (EEG), Multivariate Measures (MM), Synchronization.

I. INTRODUCTION

The Synchronization of brain waves is a hypothetical mechanism of functional connectivity involved in the information processing in the nervous systems [1], [2], which is altered in many brain disorders, including schizophrenia [3],Alzheimer's disease [3], [4], epilepsy [5]–[7],Parkinson's disease [8], and autism [9]. Electroencephalogram (EEG) has been frequently used to study synchronization in the brain. EEG is also the prime technique for various applications in brain–computer interface studies [10]–[12] due to its low-cost and easy-to-use architecture.

Techniques available in signal processing and dynamical systems have a long history of applications to EEG. Early studies were based on a few EEG signals evaluated with spectral analysis including power spectral density and coherence [13]–[15]. Other bivariate techniques for assessing functional connectivity via synchronization have also been used. These include cross- correlation, mutual information, synchronization likelihood, and phase locking [5], [16]–[18]. Modern multichannel EEG techniques allow the reconstruction of distributed sources in the brain with relatively fine spatial resolution [5], [16]–[18], which suggests new options for synchronization analysis, for instance, detailed 3-D whole-brain mapping by means of multivariate synchronization techniques [4], [19]–[21]. Such mapping has a promise to become an effective instrument of clinical neuroscience by providing the disease specific patterns of synchronization [3], [4], [19], [22], [23]. Furthermore, synchronization in the brain can be a consequence of different processes [24], [25]. Thus, different experimental designs or clinical conditions might require measures sensitive to different synchronization profiles.

Here, we provide a review of bivariate and multivariate synchronization measures and supplement it by their application to multivariate EEG time series. Bivariate measures (cross correlation, coherence, phase locking value, and mutual information) result in synchrony estimation for a pair of sensors. In order to obtain a single metric for the synchrony within a region including more than two sensors, these values are averaged over all possible pairs in the region. In contrast, multivariate measures (such as multivariate phase synchronization, global field synchronization, omega complexity, and state -space based estimators) provide a direct synchrony value for multivariate recordings. The aim of this analysis is to determine the common and unique properties of various synchronization measures, thus allowing a researcher to select the one best addressing a specific research issue of interest in experimental and clinical neuro science. To this end,

synchronization measures are assessed and compared using both artificially generated time series (through coupled non identical Rössler and Colpitts oscillators) and real EEG recordings from healthy adult subjects.

II. Synchronization Measures

Let us start with a multivariate measurement $\mathbf{Y}$ that is an N-variate time series as

$$\mathbf{Y} = \{Y_i^t\}; \quad t = 1, 2, \ldots, L; \; i = 1, 2, \ldots, N$$

where $Y_t \in \mathbb{R}_N$ is the tth sample observation vector of the ith time series and L is the number of available samples. Indeed, $\mathbf{Y}$ is an $N \times L$ matrix whose rows correspond to the univariate time series of length L.

The synchrony level of $\mathbf{Y}$ can be estimated in two ways. One way is to use conventional bivariate measures and to calculate all pair-wise synchronization indexes, resulting N (N – 1) / 2 values. These values are then averaged to find a mean synchrony level for N time series. An alternative is to use direct estimation of synchrony within multivariate time series. In this work, both approaches are reviewed and applied to artificially generated data and real EEGs.

A. Bivariate Synchrony Measures

For this type of indexes, the key point is to measure the amount of synchrony between two time series. To this end, one may use linear or nonlinear, time-domain or frequency-do-main interdependency measures. Here, we review a number of bivariate measures that are often used to calculate the interdependency between two time series Y_1 and Y_2.

1) Cross Correlation: Cross correlation is a simple synchrony measure that is frequently used for capturing linear interdependencies in time domain. The Pearson product-moment correlation coefficient between Y_1 and Y_2 is calculated as

$$\mathrm{Corr}_{Y_1,Y_2} = \frac{\sum_{t=1}^{L}\left(Y_1^t - \frac{1}{L}\sum_{t=1}^{L} Y_1^t\right)\left(Y_2^t - \frac{1}{L}\sum_{t=1}^{L} Y_2^t\right)}{\sqrt{\sum_{t=1}^{L}\left(Y_1^t - \frac{1}{L}\sum_{t=1}^{L} Y_1^t\right)^2}\sqrt{\sum_{t=1}^{L}\left(Y_2^t - \frac{1}{L}\sum_{t=1}^{L} Y_2^t\right)^2}}. \quad (2)$$

2) Cross Coherence: Correlation is a measure in time do-main. In order to obtain the dependency in a certain frequency band, the data should be filtered in that band and the correlation coefficient computed for the filtered data. An alternative is to use cross coherence analysis. To this end, first, the data is trans-formed to frequency domain by means of fast Fourier transform. The cross coherence of two signals Y_1 and Y_2 at frequency f is obtained as,

$$\mathrm{Coh}_{Y_1,Y_2}(f) = |P_{Y_1Y_2}(f)|^2 \Big/ \left(|P_{Y_1Y_1}(f)|\,|P_{Y_2Y_2}(f)|\right) \quad (3)$$

where P_{Y1Y2} is cross power spectral density at frequency f. The coherence at a certain frequency band can be obtained by averaging above values over that range.

3) Mutual Information: Mutual information (MI) is a measure of nonlinear relationship between two time series. In order to compute MI, the time series Y_1 and Y_2 are considered to be realizations of two stochastic processes with M possible out-comes, which can be obtained by partitioning the time series into M bins. For each of these outcomes, a probability distribution should be calculated. Finally, the MI is computed as

$$\mathrm{MI}_{Y_1,Y_2} = \sum_{i=1}^{M}\sum_{j=1}^{M} P_{Y1,Y2}^{i,j} \ln \frac{P_{Y1,Y2}^{i,j}}{P_{Y1}^{i} P_{Y2}^{j}} \quad (4)$$

Where $P_{Y1,Y2}^{i,j}$ is the estimated joint probability of the outcomes i and j for the time series, and P_{Y1}^{j} is the estimated probability distribution of jth outcome of time series Y_1. The MI between two time series measures how different is the true joint probability distribution from the joint probability distribution of two independent time series.

4) Phase Locking Value: When applied to the original time series, the metrics described above depend on the amplitudes of the signals. In some applications, one might be interested in a measure, which is independent of the amplitude. One possible solution is to estimate the phase synchrony. In computing the phase locking value (PLV) between two time series, the first step is to extract the instantaneous phases out of the time series. Usually, Hilbert transform is used to this end. Considering a univariate time series Yt, and its Hilbert transform as Yt [26], the instantaneous phase of the time series Y_i is obtained as [11], [27]

$$\varphi_i^t = \arctan\left(\bar{Y}_i^t \Big/ Y_i^t\right). \quad (5)$$

Two oscillators are phase synchronized, if their phases are locked to each other, i.e., the difference of their phases does not change over time. In order to quantify how well two time series are phase locked, one can use the following metric [11]

$$\mathrm{PLV}_{Y_1,Y_2} = \frac{1}{L}\left|\sum_{t=1}^{L} e^{j(\varphi_1^t - \varphi_2^t)}\right|. \quad (6)$$

where j is the imaginary unit.

B. Multivariate Synchrony Measures

An approach to compute synchronization within multivariate time series is to consider all the series as components of a single interdependent system and to use multivariate measures. A number of multivariate synchrony measures reviewed here have been introduced in the literature and successfully applied to real EEGs.

1) Omega Complexity: An N-variate time series can be viewed as a representation of trajectories that can be modeled in

N-dimensional state- space. Omega complexity assesses the dimensionality of these trajectories in the state-space based on principal component analysis. Let $\boldsymbol{C}=(C_{ij})$ be the covariance matrix, in which the entry C_{ij} is the cross-correlation between the time series i and j calculated from (2). Using the eigen values of the correlation matrix $\boldsymbol{C}$ as $\lambda(i=1,2,N)$, we compute the omega complexity as in [28]

$$\Omega = \exp\left(-\sum_{i=1}^{N} \frac{\lambda_i}{N} \log \frac{\lambda_i}{N}\right). \quad (7)$$

Omega complexity Ω varies between 1 (maximum synchronization) and N (minimum synchrony, i.e., maximum de-synchronization). In order to scale the above measure between a value close to 0 (for minimum synchrony) and 1 (for maximum synchrony), one can compute Omega as

$$\text{Omega} = 1/\Omega. \quad (8)$$

Omega will be $1/N$ for no-synchrony cases, which is close to zero for large N. The omega quantifies the amount of synchronization for a dataset by comparing the actual dimensionality of the network with the expected full dimensionality of the asynchronous network. Let us consider a system composed of two coupled pendula, where each pendulum can be fully de-scribed by two differential equations. If the pendula are not coupled, they have independent motion, resulting in a four dimensional system. If they get into full harmony through coupling, the system can be regarded as a single pendulum, and thus, the dimensionality will be two.

2) S-Estimator: The State-Space (S) estimator is an extension to omega complexity based on Shannon entropy. The S-estimator is obtained as

$$\text{SS} = 1 + \frac{\sum_{i=1}^{N} \frac{\lambda_i}{N} \log\left(\frac{\lambda_i}{N}\right)}{\log(N)}. \quad (9)$$

The S-estimator indirectly measures the synchronization induced contraction of the embedding dimension in state-space [19] by determining the entropy of the eigen values of the correlation matrix$\boldsymbol{C}$. The minimum entropy characterizes the situations when few normalized eigen values are nonzero, while others are close to zero. In such situations, the S-estimator is close to 1, showing the high levels of synchronization. When synchrony within the system is weak, many eigen values are the same, resulting in the maximum entropy and S-estimator close to 0.

3) S-Estimator Based on Renyi Entropy: An extension of S-estimator based on Renyi entropy is a more reliable measure of multivariate synchronization [29]. It is calculated as

$$S - \text{Renyi} = 1 + \frac{1}{(\alpha-1)\log(N)} \log \sum_{i=1}^{N} (\lambda_i/N)^{\alpha}. \quad (10)$$

The Renyi entropy approaches to Shannon entropy, when α goes to 1. S-Renyi can be fine tuned by controlling α, and it was shown that the value of $\alpha=6$ results in an unbiased dependency measure showing the most similar behavior to simple Pearson correlation for two time series [29]. It was also shown that S-estimator based on Renyi entropy is more robust and less sensitive to noise than conventional S-estimator.

4) Multivariate Phase Synchronization: Omega complexity, S-estimator and S-Renyi are all based on covariance matrix. In other words, these metrics estimate linear relationship among the times series. Similar to bivariate measures such as correlation and coherence, they suffer from dependency on the amplitude of the oscillations. This might bias the outcome, if the aim is to find an amplitude-independent synchrony within systems. A solution to this problem is to use multivariate phase synchrony (MPS) measure, which is indeed an extension to PLV as expressed in (6). Having extracted the instantaneous phases from the individual time series (using the Hilbert transform, for instance), the MPS is computed as

$$\text{MPS} = \frac{1}{LN} \sum_{t=1}^{L} \left| \sum_{i=1}^{N} e^{j\varphi_i(t)} \right|. \quad (11)$$

MPS measures the mean phase coherence between the time series, averaged over the observation samples. It ranges from 0 for completely non phase synchronized systems to 1 for completely phase-synchronized systems.

5) Global Field Synchronization: A multivariate synchronization can be calculated in frequency domain by means of global field synchronization (GFS) measure [30]. First, the time series are converted to frequency-domain using fast Fourier transform. This results in the *sine* and *cosine* coefficients. At a given frequency f, the multivariate signals can be visualized in two-dimensional *sine-cosine* maps. As the entries are getting more scattered, the phase synchrony between them worsens. Let $\lambda_1(f)$ and $\lambda_2(f)$ be the eigen values of the covariance matrix along these two vectors (coefficients of *sine* and *cosine*). GFS at a given frequency f is calculated as

$$\text{GFS}(f) = \frac{|\lambda_1(f) - \lambda_2(f)|}{\lambda_1(f) + \lambda_2(f)}. \quad (12)$$

If the *sine-cosine* clouds lie on a straight line, one of the eigen values equals to 0 and the covariance is completely explained by a single principal component; the GFS takes a value of 1 for such cases. This corresponds to complete phase synchrony at a given frequency. In a non phase-synchronized case, the two eigen values are close to each other, leading to GFS values close to 0. In order to obtain GFS values in a certain

frequency range, similar to cross-coherence, one can get the average of GFS values over that frequency range.

In this work, we do not consider the extension of synchronization measures for delay-embedded time series [31]. How-ever, the multivariate estimators reviewed can be extended to assess delay embedding in the time series, i.e., lagged systems, which would be especially interesting in the light of the recent theoretical analysis of a role of delays in network synchronization [32]–[35].

Next, we evaluate the behavior of these measures in both artificially generated time series and real EEGs.

III. Numerical Assessment Based On Coupled Oscillators

To study the synchrony measures as a function of coupling strength, connection density, and of parameter mismatch between the individual oscillators, we exploited the time series obtained through numerical simulations. In order to produce time series with varying levels of synchrony between them, we used coupled non identical Rössler [36] and Colpitts [37] oscillators. These systems produce irregular sine-like waves similar to the EEG, and have been previously utilized for validating synchrony measures [19]. The equations of the Rössler oscillator is given by [36]

$$\begin{cases} \dot{x} = -\omega y - z \\ \dot{y} = \omega x + a y \\ \dot{z} = d + z(x - c) \end{cases} \quad (13)$$

Where (x ,y, z) define the states of the oscillator, ω is the natural frequency of the oscillator, and a ,d , and c are parameters characterizing its behavior.

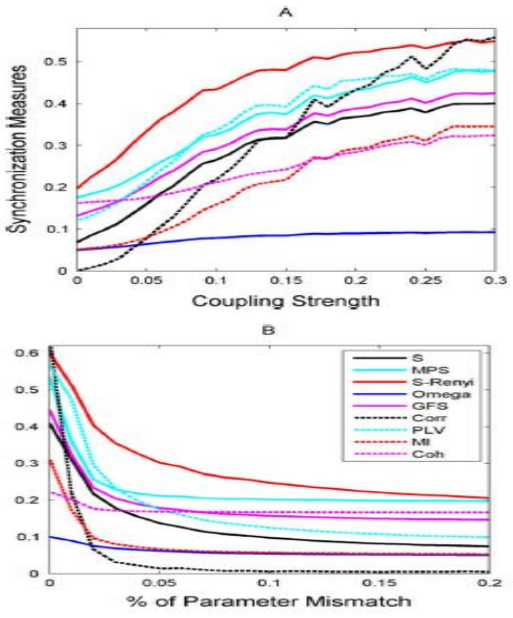

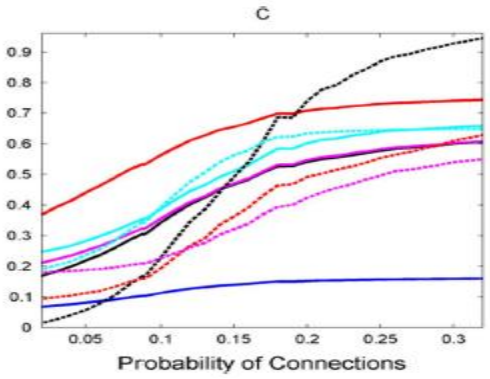

Fig. 1. Various synchronization measures as a function of (A) coupling strength, (B) % of parameter mismatch, and (C) probability of connection in Erdos-Renyi networks P when the individual dynamical systems are chosen as Rössler oscillator. In each case, only one parameter changes and the other two are fixed. The connection networks were Erdos-Renyi with N=25 nodes and the measures were calculated within all 25 nodes with dynamics as expressed by (12). The graphs show averages over 200 realizations. The studied synchronization measures are coherence (Coh), mutual information (MI), phase locking value (PLV), correlation (Corr), generalized field synchronization (GFS), Omega, multivariate phase synchronization (MPS), S-estimator S , and S-estimator based on Renyi entropy (S-Renyi).

In a network with N nodes, nodes represent individual oscillators, and links represent coupling between them. Let us consider coupling through the x-state between the oscillators. The equations of the motion of coupled oscillators read

$$\begin{cases} \dot{x}_i = -\omega_i y_i - z_i + \sigma \sum_{j=1}^{N} A_{ij}(x_j - x_i) + R \\ \dot{y}_i = \omega_i x_i + a_i y_i \\ \dot{z}_i = d_i + z_i(x_i - c_i) \end{cases} \quad i = 1, \ldots, N \quad (14)$$

Where A=(A_{ij})is the adjacency matrix of the connection graph, R is the noise, and σ is the unified coupling strength between the oscillators.

The nominal parameters of the oscillators were set a ω=1, a=0.165, d=0.2 and c=10. Furthermore, we considered 10% mismatch between the parameters of oscillators, i.e., the case of non identical oscillators. The noise level was fixed at R=0.02. The Colpitts oscillators are also connected through their x-components. The individual dynamics of Colpitts systems is

$$\begin{cases} \dot{x}_i = \frac{g}{Q(1-k)}(\alpha(e^{-y} - 1) + z) \\ \dot{y}_i = \frac{g}{Qk}((1-\alpha)(e^{-y} - 1) + z) \\ \dot{z}_i = -\frac{Qk(1-k)}{g}(x + y) - \frac{1}{Q}z \end{cases} \quad (15)$$

where the parameter values were chosen as k=0.5,g in the

range of [4, 4.4],Q in the range of [1.34, 1.48], and α in the range of [0.94, 1].

As a connection structure, we considered random Erdos Renyi (ER) networks with [38]. In such networks, between any pair of nodes there is a link with probability P (was used in this work). The networked differential equations were iterated, using the Heun algorithm [39], starting from random initial conditions. We considered the simulation time units and the integration time-step. The time series of x-components were segmented into 25 epochs of equal length, while a number of initial iterations was neglected in order to eliminate transients. Then, the synchrony measures were calculated separately for each epoch and, finally, averaged over all of them. The numerical simulation ran for 200 times (each time for a different random network with the same and independent initial conditions) and the results were averaged over all realizations.

In this work, we used simulated time series with known parameters to verify whether any synchronization measure(s) can capture them. To this end, we set the parameters such that in-creasing the coupling strength between the individual oscillators would improve their synchrony. Then, we assessed how different estimators reflect this effect. Rössler oscillator may undergo a desynchronized regime by increasing the coupling strength over a certain threshold. In this connection, through the master stability function approach [40], we chose the parameters such that the gradient of the Lyapanov exponent remained negative with increasing coupling strength, thus keeping the system in synchronized regime. Therefore, in our setting, the synchrony always increased with the coupling strength.

Fig. 1 shows the behavior of synchrony measures for coupled Rössler oscillators as a function of coupling strength, mismatch in parameters, and the probability of connections (P) in ER networks. In each panel of this figure, only one parameter (connection strength, mismatch, or P) changes, while the other two are fixed. All the measures show the same trend: they in-crease with coupling strength, increase as P increases (the net-works become denser), and decrease as the mismatch of individual parameters increases. However, their profiles differ: Omega shows the least changes with the changes of the parameters, whereas Corr shows the most pronounced changes. S-Renyi has the highest value in the most of cases followed by MPS and PLV.

In order to compare different synchrony measures in terms of their profiles against different settings (e.g., their behavior as a function of coupling strength), we used an index of their

TABLE I
MEAN VALUES AND STANDARD DEVIATIONS OF THE MONOTONICITY PARAMETER (*M*) FOR THE SYNCHRONIZATION MEASURES IN DIFFERENT SETTINGS.OTHER DESIGNATIONS ARE AS IN FIG. 1 FOR RÖSSLER OSCILLATOR AND FIG. 2 FOR COLPITTS OSCILLATOR

Setting/synchronization measure	Corr	Coh	MI	PLV	MPS	GFS	Omega	S	S-Renyi
Coupled Rössler Oscillators									
Coupling Strength	0.64±0.07	0.69±0.06	0.66±0.06	0.61±0.07	0.65±0.07	0.67±0.06	0.66± 0.06	0.66± 0.06	0.66±0.07
Probability of Connections	0.82±0.03	0.85±0.03	0.84±0.03	0.81±0.04	0.82±0.03	0.78±0.04	0.85±0.03	0.85±0.03	0.83±0.03
% of Parameter Mismatch	-0.37±0.15	-0.66±0.08	-0.76±0.06	-0.88±0.04	-0.58±0.10	-0.78±0.06	-0.83±0.05	-0.83±0.05	-0.78±0.06
Coupled Colpitts Oscillators									
Coupling Strength	0.61±0.06	0.67±0.07	0.60±0.06	0.55±0.07	0.57±0.07	0.55±0.08	0.61±0.06	0.61±0.06	0.61±0.06

Monotonic behavior [41]. Let us consider a Synchrony Measure (SM) as a function of coupling strength, which takes values in n points. The degree of monotonicity M is defined as

$$M = \frac{2}{n(n-1)} \sum_{i=1}^{n-1} \sum_{j=i+1}^{n} \text{sign}(\text{SM}_j - \text{SM}_i) \qquad (16)$$

Where sign (.) stands for the sign (+1 or -1) of the term and M captures the monotonic behavior of synchrony measures. M=1 indicates a strictly increasing sequence for SM, whereas M= -1 shows a strictly decreasing pattern. Any value between these two extremes estimates the monotonicity of specific SM. M shows the sensitivity of a synchrony measure to the variations of real functional connectivity. Since functional connectivity increases with coupling strength, an SM with the highest M value would be the most sensitive for capturing the changes in functional connectivity.

Table I shows the values of the monotonicity parameter (M) of the synchronization measures in different settings. The positive values of M for increasing the coupling strength and connection probability and negative M for increasing the parameter mismatch are expected. Although all synchrony measures show monotonic behavior, the degree of monotonicity is different. Not a single measure is the most sensitive one in all settings. Coh shows the highest sensitivity to (linear) coupling strength and connection probability. When the mismatch of parameters changes, PLV shows the highest sensitivity, whereas Corr demonstrates the least sensitivity. The latter setting is different from the first two settings in that its effect on the functional connectivity is nonlinear. That is why the linear measures Corr and Coh show less sensitivity to the changes in the mismatch parameter compared to MI that is able to capture non-linear interactions.

Fig. 2 shows a trend of synchronization among coupled Colpitts oscillators as a function of coupling strength. All measures

mirrored the scalability of synchronization with the coupling strength and the results are similar to those from Rössler oscillators. Specifically, for both oscillator types, Omega resulted in the least values, while S-Renyi resulted in the highest values. Table I shows that the sensitivity of the measures with respect

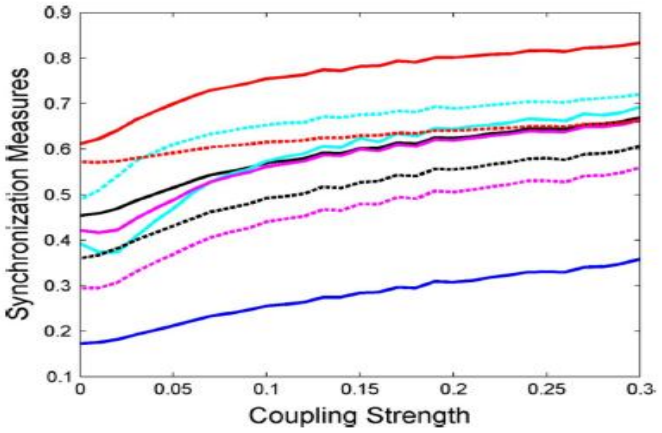

Fig. 2. Various synchronization measures as a function of coupling strength in coupled Coliptts oscillators. Other designations are as Fig. 1.

to the coupling strength are similar for Colpitts and Rössler systems. In both cases, Coh showed the highest sensitivity against coupling strength, while PLV was the least sensitive measure. Next, we examined these measures in real EEGs of a number of healthy subjects.

IV. Application To Real EEG

A. EEG Recording and Preprocessing

The synchronization measures were applied to the EEGs recorded from 20 neurologically healthy subjects, which participated as controls in our studies of synchronization abnormalities in Alzheimer's disease and psychogenic non epileptic seizures [4], [23], [42], [43]. All the subjects gave written informed consent. All the applied procedures and research methods conform to the Declaration of Helsinki (1964) by the World Medical Association concerning human experimentation and were approved by the local Ethics Committee of Lausanne University. The EEG data were collected while subjects were seated relaxed with eyes closed in the EEG laboratory of the Department of Neurology, Centre Hospitalier Universitaire Vaudois (Lausanne, Switzerland). The EEGs were recorded with the 128-channel Geodesic Sensor Net (EGI, Inc., Eugene, OR, USA) for 3–4 min (Fig. 2). The sensors located in the outer ring of the montage (18 sensors) were removed from further analysis because of low signal- to-noise ratio. All electrode impedances were kept under 50 k Ω as required for the high - input-impedance amplifiers. The recordings were made with vertex reference using a low-pass filter set to 100 Hz. The signals were digitized at a rate of 500 samples/s with a 12 -bit analog - to-digital converter and filtered (FIR, band-pass of 1–50 Hz). Artifacts in all channels were edited offline: first automatically, based on an absolute voltage threshold (100 μ V) and on a transition threshold (50 μ V sample-to-sample), and then on the basis of a thorough visual inspection. The sensors producing artifacts more than 20% of the recording times were corrected with a bad channel replacement tool (Net Station 4.2, Electrical Geodesic Inc., OR, USA). To obtain the high confidence synchronization estimates, the signals were segmented into non overlapping 1- s epochs. The number of artifact- free epochs entered into the analysis was 176 ± 57 per subject. The analysis was performed in conventional EEG frequency bands including delta (1–3 Hz), theta (3–7 Hz), alpha (7–13 Hz), beta (13–30 Hz), and gamma (30–50 Hz). To minimize the unwanted effects of volume conduction on synchronization estimates, we used the high-resolution Laplacian transformed EEG signals [44]. In order to filter the EEGs and to compute the Laplacians, we used EEGLAB [45] and CSD [46] toolboxes available from MATLAB packages.

B. Assessment of the Whole-Head Topography of Synchronization

In order to calculate the whole- head synchronization maps, first, EEGs were mean detrended and normalized to unitary variance, thus diminishing the influence of the variations of EEG amplitude. Then, the data were filtered for the specific frequency band. For each sensor, a region including the sensor itself and its first neighbors was considered (Fig. 3). The choice of neighborhood allows estimating multivariate regional synchronization locally/regionally. From anatomical perspective, this is an intra- and inter-areal synchronization presumably mediated via the short association fibers. In contrast to the analysis of long-distance synchronization, this approach is optimal for the whole -brain (whole-head) mapping of functional connectivity (for discussion see [4], [23], [42], [43]) . Indeed, recent research demonstrated the patterns of regional synchronization specific for diseases affecting the brain at a systems level, including such dissimilar conditions as Alzheimer's disease [4], psychogenic non epileptic seizures [23], and schizophrenia [22]. The synchronization maps were constructed by averaging all pair-wise bivariate measures (Corr, Coh, MI, and PLV) and by computing sensor- wise the multivariate measures (Omega, S-estimator, S-Renyi, MPS, and GFS) over respective region.

C. Correlation Analysis

We calculated the sensor-wise Pearson correlation coefficients between the synchronization measures. The P-values

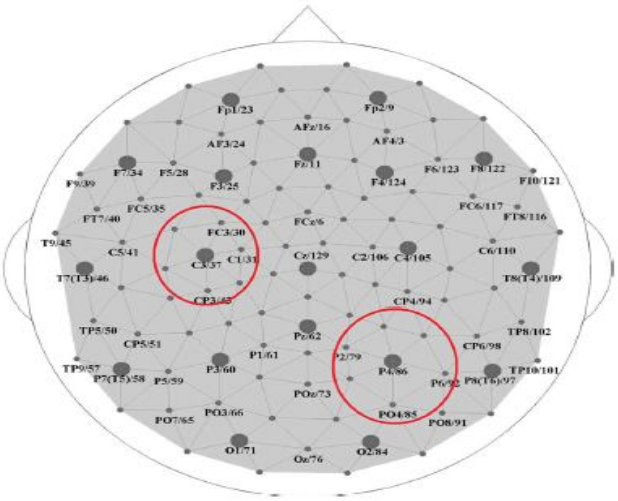

Fig. 3. Diagram shows the correspondence between the high-density 129-channel Sensor Net (EGI, Inc.,) and the International 10-10 System. 18 sensors in the outer rings are removed from further processing due to low signal-to-noise ratio. The sensor locations encircled in red exemplify the first neighborhood for the sensors 37 and 86, i.e., the territory considered for the calculation of a single value of synchronization measures. The obtained synchronization values can be accounted as regional synchrony among neigh-boring sensors.

were corrected using the false discovery rate method proposed by Benjamin and Hochberg (BH) [47] to account for multiple comparisons. Significant correlations with $P<005$ (BH corrected) are presented.

D. Results and Discussion

We were mainly interested to assess whether there are systematic differences between the outcomes of bivariate and multivariate measures and whether the (dis) similarities between the synchrony measures are frequency specific. Fig. 4 shows the synchronization maps for conventional frequency bands based on different bivariate and multivariate measures. Since these metrics estimate different aspects of the synchronization process, it is not surprising that the synchrony level is different across different metrics and frequency bands. For example, on average, S-Renyi resulted in the highest level of regional synchrony, while MPS, in the lowest one.

Table II shows a percentage of sensors with significant correlations ($P<005$, BH corrected) between the analyzed synchrony measures. The correlation maps for the main EEG frequency bands are presented in the supplementary file. These maps are almost frequency -independent across all metrics but Coh, for which the number of sensors showing significant correlation with other metrics in gamma band is considerably lower than in other frequency bands.

Corr, Omega, S-estimator, and S-Renyi show significant inter-correlations across all frequency bands and EEG sensor locations. Furthermore, other synchronization measures (except Coh) similarly correlate with these four metrics. Among them,

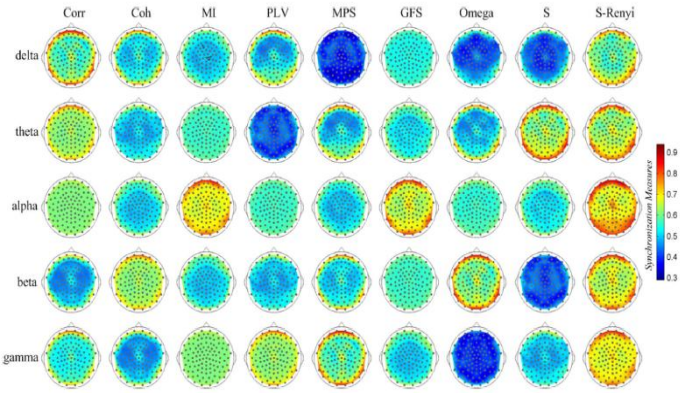

Fig. 4. Group-averaged synchronization maps based on various metrics in conventional frequency bands including delta (1–3 Hz), theta (3–7 Hz), alpha (7–13 Hz), beta (13–30 Hz), and gamma (30–50 Hz). For designations of the metrics see Fig. 1.

Corr is a bivariate measure and the other three are multivariate measures that are obtained through eigen-decomposition of correlation matrix. Therefore, eigen value decomposition has a little effect on cross-correlation values and the synchronization measures based on correlation matrix are similar to cross-correlation. PLV and MI are also highly correlated with Corr, Omega, S-estimator, and S-Renyi across all frequency bands (except correlations between MI and other five metrics in delta band).

As a multivariate measure of phase synchronization, MPS shows correlations with Corr, MI, PLV, Omega, S-estimator, and S-Renyi, predominantly over occipital and parietal areas of the brain. These correlations are stronger in theta and beta bands. Interestingly, PLV- and

TABLE II

TABLE REPRESENTS PERCENTAGE OF SENSORS SHOWING SIGNIFICANT CORRELATION (P< 0.05 BH CORRECTED) BETWEEN DIFFERENT SYNCHRONIZATION MEASURES. THE CORRELATION VALUES ARE (FROM LEFT TO RIGHT) FOR DELTA, THETA, ALPHA, BETA, AND GAMMA BANDS

	Corr	Coh	MI	PLV	MPS	GFS	Omega	S	S-Renyi
Corr		67,82,99,80,10	69,99,100,100,100	99,100,98,100,100	66,73,77,87,68	3,2,0,0,6	all 100	all 100	all 100
Coh	67,82,99,80,10		18,49,98,78,9	50,74,100,78,11	67,52,99,55,10	67,0,99,0,10	63,84,100,76,7	66,84,100,76,8	68,84,97,81,14
MI	69,99,100,100,100	18,49,98,78,9		90,97,96,100,100	26,54,64,78,61	3,1,5,1,11	73,97,100,100,100	74,96,100,100,100	74,96,100,100,100
PLV	99,100,98,100,100	50,74,100,78,11	90,97,96,100,100		51,71,55,86,65	0,2,5,0,5	99,100,100,100,100	99,100,100,100,100	99,100,95,100,100
MPS	66,73,77,87,68	67,52,99,55,10	26,54,64,78,61	51,71,55,86,65		1,0,0,0,2	53,58,62,74,54	57,59,63,76,57	67,74,80,87,75
GFS	3,2,0,0,6	67,0,99,0,10	3,1,5,1,11	0,2,5,0,5	1,0,0,0,2		11,11,10,5,12	10,8,8,5,12	5,1,0,0,6
Omega	all 100	63,84,100,76,7	73,97,100,100,100	99,100,100,100,100	53,58,62,74,54	11,11,10,5,12		all 100	all 100
S	all 100	66,84,100,76,8	74,96,100,100,100	99,100,100,100,100	57,59,63,76,57	10,8,8,5,12	all 100		all 100
S-Renyi	all 100	68,84,97,81,14	74,96,100,100,100	99,100,95,100,100	67,74,80,87,75	5,1,0,0,6	all 100	all 100	

MPS-based maps are characterized by widespread insignificant correlations, especially, in delta and alpha bands. Both MPS and PLV are estimators of phase synchrony between the time series; however, their properties are different.

Among the synchronization measures, GFS shows the least correlation with others. Except for its correlations with Coh in delta and alpha bands, there are almost no significant correlations with other metrics in any band. Our numerical simulations show that GFS has a relatively high sensitivity to functional connectivity of network (Table I). At a given frequency, GFS measures the relative absence or presence of a common phase over the group of sensors or sources (the first neighbors here). The GFS values can be interpreted as the maximum power that can be explained by a single phase. As can be seen from the correlation maps, synchronization process captured by GFS is fundamentally different from those explained by Corr, MI, Omega, S-estimator, and S-Renyi.

It is worth mentioning that Laplacian transform, used here to reduce the volume conduction effects in EEG, is selectively sensitive to shallow cortical potentials and not unbiased with respect to performance of amplitude-sensitive and phase-sensitive synchrony measures. While being sufficient for the comparison between bivariate and multivariate measures, it is suboptimal for the functional connectivity studies in human neuroscience, which require an analysis in EEG source space.

V. Conclusion

EEG is frequently used for studying brain activity in normal individuals and in patients with various psychiatric and neurological disorders. Availability of modern multichannel/multi-source EEG calls for the appropriate methods of the analysis of multivariate time series, including their synchronization, which is in the heart of the most accepted hypothesis of information processing in the central nervous system. In this paper, we re-view the state of art in multivariate synchronization analysis and compare various synchronization measures applied to the time series obtained via numerical simulations and to real EEG. We divide the estimators of synchronization into bivariate and multivariate. Bivariate measures include estimators, which must be averaged over all pairs of signals in the region of interest to obtain a multivariate synchrony value. The multivariate measures directly estimate a single value for multivariate time series. Here we applied bivariate and multivariate methods to simulated data as well as to Laplacian transformed EEGs from a group of healthy subjects. Although these methods capture different features of the synchronization process, many of them show significant correlations across the whole-head synchronization maps.

Except Coh that shows a frequency dependent correlation with other metrics, the synchrony measures analyzed here demonstrate almost a frequency-independent behavior. Those measures that are highly correlated across all frequency bands (S-estimator, S-Renyi, Omega, and Corr) can be equally used. Some of the measures are more sensitive to linear interdependences (S- estimator, S-Renyi, Omega, Corr, and Coh), whereas others are more sensitive to nonlinear effects (MI, PLV, MPS, and GFS), thus providing complementary information. We observed high correlations between many of bivariate or multivariate synchronization measures indicating that they similarly estimate the same synchronization phenomenon. Therefore, in terms of output, multivariate measures do not have superiority over bivariate ones. However, since multivariate measures are computationally efficient and can be effectively applied to large-scale data sets, they should be preferred to bivariate measures in such datasets.

References

[1]. J. Lisman and G. Buzsaki, "A neural coding scheme formed by the combined function of gamma and theta oscillations," *Schizophrenia Bull.*, vol. 34, pp. 974–980, 2008.

[2]. J. Fell and N. Axmacher, "The role of phase synchronization in memory processes," *Nat. Rev. Neurosci.*, vol. 12, pp. 105–118, 2011.

[3]. M. G. Knyazeva, C. Carmeli, A. Khadivi, J. Ghika, R. Meuli, and R.S.Frackowiak, "Evolution of source EEG synchronization in early Alzheimer's disease," *Neurobiol. Aging*, vol. 34, pp. 694–705, 2013.

[4]. M. G. Knyazeva, M. Jalili, A. Brioschi, I. Bourquin, E. Fornari, M. Hasler, R. Meuli, P. Maeder, and J. Ghika, "Topography of EEG multivariate phase synchronization in early Alzheimer's disease," *Neurobiol. Aging*, vol. 31, pp. 1132–1144, 2010.

[5]. V. Sakkalis, C. D. Giurcaneanu, P. Xanthopoulos, M. E. Zervakis, V.Tsiaras, Y. Yang, E. Karakonstantaki, and S. Micheloyannis, "Assessment of linear and nonlinear synchronization measures for analyzing EEG in a mild epileptic paradigm," *IEEE Trans. Inf. Technol. Biomed.*, vol. 13, no. 4, pp. 433–441, Jul. 2009.

[6]. K. Ansari-Asl, J.-J. Bellanger, F. Bartolomei, F.Wendling, and L.Senhadji, "Time-frequency characterization of interdependencies in nonstationary signals: Application to epileptic EEG," *IEEE Trans. Biomed. Eng.*, vol. 52, no. 7, pp. 1218–1226, Jul. 2005.